Full-tensor alignment criteria for sheared nematic polymers

M. Gregory Forest and Ruhai Zhou
Department of Mathematics
University of North Carolina at Chapel Hill
Chapel Hill, NC 27599-3250

Qi Wang
Department of Mathematics
Florida State University
Tallahassee, FL 32306

September 22, 2002

Synopsis

The shear problem for nematic polymers consists in characterizing all stable stationary orientational distributions, steady and unsteady, versus shear rate and nematic concentration (cf., [Marrucci and Greco (1993)]). Specific features, e.g., the primary alignment angle and normal stress differences of steady states, further characterize nematic polymers in simple shear. Leslie-Ericksen (L-E) theory provides *formulas* for the shear response of liquid crystals, in terms of a Leslie viscosity ratio. The analogous result for mesoscopic and kinetic theory of nematic polymers is the topic of this paper. Kuzuu and Doi (1983, 1984) developed a weak-flow limit of kinetic theory, which reproduces L-E theory and gives a molecular basis for continuum parameters. Their method does not aim to capture further rheological features of the weak-shear response: the total number of stationary distributions and their stability; the spreading or biaxiality of each distribution; in-plane to out-of-plane transitions; and normal stress differences and shear stress for each stable steady distribution. These features of kinetic theory are only accessible by numerical simulations (cf. [Larson (1990), Larson and Ottinger (1991), Faraoni *et al.* (1999)]), from which multi-parameter scaling properties of steady attractors remain elusive. In this paper we develop an extension of the Kuzuu-Doi asymptotic method applicable to any mesoscopic tensor model, which yields all steady-state features listed above, explicitly in terms of mesoscopic theory parameters. The mesoscopic solvability conditions reduce to linear algebra, and can be carried to any order in the shear-rate expansion. To illustrate, we explicitly solve the steady weak shear problem for the Doi quadratic closure model, whose parameters are nematic concentration N and molecular aspect ratio r. Formulas for alignment angles and rheological features of all stable steady states are derived and graphed to show scaling behavior versus N and r. The parameter regions (N, r) of unsteady weak shear response are identified but transient solutions are not characterized. The theory is confirmed with numerical simulations. Our method extends recent in-plane tensor model analysis for steady states in weak shear [Wang (1997), Rienacker and Hess (1999), Maffettone *et al.* (2000), Forest and Wang (2002)].

1 Introduction

The shear problem for nematic polymers is a classical topic in rheology and nonlinear anisotropic viscoelasticity, providing an experimental test bed for theory as well as a theoretical framework for experiments (cf., [Kuzuu and Doi (1983, 1984), Marrucci (1991), Marrucci and Greco (1991, 1993)]). The quiescent nematic liquid is isotropic below a critical concentration, then ordered along a distinguished direction: the director of Leslie-Ericksen (L-E) theory, the major director of mesoscopic tensor theory, or some measure of the peak of the probability distribution function (pdf) in kinetic theory. (The standard prescription of kinetic theory is to compute the second moment of the pdf, which defines a second-order tensor and therefore a major director.)

Absent of an applied field, the "director" is arbitrary, and the shear problem is to determine how this rotational degeneracy is broken. In weak shear, the monodomain response is not unique; the nematic liquid may be steady or unsteady, and theory aspires to distinguish this behavior depending on molecular or mesoscopic or continuum parameters. At the next level of detail, steady states may align in-plane or out-of-plane, and unsteady states may tumble in-plane or out-of-plane [Larson (1990), Larson and Ottinger (1991), Faraoni *et al.* (1999), Forest and Wang (2002), Forest *et al.* (2002a)]. Continuum theory [Marrucci and Grizzuti (1987)] provides a single and practical criterion in terms of the Leslie tumbling parameter, $\lambda_L = \frac{1+\alpha_3/\alpha_2}{1-\alpha_3/\alpha_2}$, depending only upon the ratio of two viscosity parameters α_2, α_3 of L-E theory. If $|\lambda_L| > 1$, flow-aligned steady states persist with Leslie alignment angle $\phi = \frac{1}{2}\arccos(1/\lambda_L)$; otherwise, some form of tumbling emerges with an explicit period formula. Thus, in continuum theory, the steady vs. unsteady shear response is a material property.

Kuzuu and Doi (1983, 1984) provided the key link between molecular kinetic theory and continuum theory by an asymptotic upscaling analysis in the weak-flow limit. In simple shear, their method gives λ_L in terms of molecular parameters, equation (1) below. The Kuzuu-Doi analysis *bypasses a general second-moment tensor* in their quest to recover the L-E director theory and molecular descriptions of the Leslie viscosities. Nonetheless, this kinetic-continuum link is fundamental since many experiments have been performed to rheologically characterize nematics from L-E theory. Indeed, nematic polymers are routinely classified as flow-aligning or tumbling [de Gennes and Prost (1993), Mather *et al.* (1996a, 1996b), Burghardt (1998), Larson (1999), Ugaz *et al.* (2001)], and the L-E theory and Kuzuu-Doi theory are the fundamental theoretical bases for this classification. Cocchini *et al.* (1990) derived mesoscopic formulas analogous to L-E theory for a two-dimensional, planar tensor model, and several authors [Wang (1997), Rienacker and Hess (1999), Maffettone *et al.* (2000), Forest and Wang (2002)] have recently shown how these formulas can be derived from a planar restriction of various full-tensor models in the weak shear limit. These results give a partial solution to the weak shear problem of mesoscopic theory, giving the Leslie alignment angle of in-plane nematic states and a Leslie tumbling parameter which predicts steady-unsteady transitions. Our goal is to first deduce existence of all steady states from a full-tensor solvability condition, then construct the weak-shear deformation of the orientation tensor and linearized stability by higher order solvability conditions.

The Kuzuu-Doi analysis is *first order in the shear rate*, and posits a *uniaxial* second-moment tensor, focusing on how the nematic director perturbs. By design, their method does not aim to capture further relevant aspects of the shear-induced orientational distribution functions: the number of stationary distributions versus concentration; the spreading and biaxiality of the distribution, i.e., order parameters of the second-moment tensor; the stability of each steady state; and transition phenomena (in-plane to out-of-plane and steady-unsteady) versus molecular parameters. In this paper we develop a mesoscopic analog of the Kuzuu-Doi asymptotic method, applicable to any second-moment tensor model, that gains all orientational and rheological features of weak-shear selected steady states, and their explicit dependence on mesoscopic model parameters.

We close the introduction with further comparison and contrast between our method and that of Kuzuu and Doi (1983, 1984). Their perturbation method is developed directly on the Doi kinetic equation, focusing on how the uniaxial director of the quiescent nematic is perturbed by weak flows. The leading-order kinetic solvability condition is a linearized, variable-coefficient, partial differential equation (pde), i.e., infinite-dimensional. The variable coefficient is given by the quiescent nematic distribution function ("f_0") as the argument of the linearized mean-field potential. This pde is not exactly solvable; indeed, even the variable coefficient is only known implicitly, and can only be computed numerically. Undaunted, Kuzuu and Doi (1983, 1984) used separation-of-variables to extract a perturbed equation for the uniaxial director of the quiescent nematic. They thereby accomplished two fundamental results:

- an implicit molecular basis for the Leslie tumbling parameter,

  $$\lambda_L = \frac{2S_2}{\langle g \frac{dU_0}{d\theta} \rangle}, \tag{1}$$

  where S_2 is the average of the second order Legendre polynomial, g is the solution of a variable-coefficient ordinary differential equation (see [Kuzuu and Doi (1983)]), U_0 is the excluded-volume, mean-field potential evaluated on the rotationally degenerate, equilibrium distribution function; and
- molecular-based formulas for continuum parameters (Leslie viscosities).

To get any explicit information about the full distribution, $f = f_0 + f_1 + \cdots$, i.e., all "f_0" that survive in weak shear for all values of nematic concentration and molecular aspect ratio, and their shear-dependent correction "f_1", one must resort to numerical simulations of the full Smoluchowski equation (cf. [Larson (1990), Larson and Ottinger (1991), Faraoni *et al.* (1999)]).

The method developed in this paper relies upon *three features* of the finite-dimensional mesoscopic approximation of kinetic theory. *First*, it is well-known how to solve the quiescent leading order problem, and explicitly parametrize the rotational symmetry of the nematic phases. Our first step is to use the weak shear solvability conditions to determine any and all directions, in-plane or not, which survive as steady states. *Second*, our solvability conditions are algebraic linear systems, and can be easily extended to any order to gain detailed information about the shear-selected stationary distributions, including the stability of each persistent state. *Finally*, the solvability conditions are indeed solvable, which we illustrate with the Doi closure model.

We thereby provide explicit formulas that convey orientational and rheological properties of all stable flow-aligned states, and their phase transitions (in-plane to out-of-plane, and steady-unsteady). The formulas are explicit, so that all properties are given in terms of the Doi theory parameters, nematic concentration N and molecular aspect ratio r. This achieves a mesoscopic version of the results that motivated Kuzuu and Doi. These predictions and scaling properties are complementary to standard experimental data, which are almost exclusively reported for a fixed nematic liquid (e.g., PBLG [Moldenaers and Mewis (1993)] or 5CB [Mather *et al.* (1996a)]) over a range of shear rates. It is significantly more challenging to vary the molecular aspect ratio (e.g., comparing 5CB and 8CB [Mather *et al.* (1996b)]), and more time consuming to vary nematic concentration (or temperature). The weak-shear analysis given here yields precisely these scaling properties of the orientation distribution and rheological features.

2 The Doi second-moment model

Let $f(\mathbf{m}, t)$ be the orientational probability distribution (pdf) function for axisymmetric ellipsoidal molecules with axis of symmetry $\mathbf{m}$ and aspect ratio r. The Smoluchowski equation for $f(\mathbf{m}, t)$ is [Doi (1981), Kuzuu and Doi (1983, 1984)]:

$$\begin{aligned} &\tfrac{Df}{Dt} = \mathcal{R} \cdot [D_r(\mathbf{m})(\mathcal{R} f + \tfrac{1}{kT} f \mathcal{R} V)] - \mathcal{R} \cdot [\mathbf{m} \times \dot{\mathbf{m}} f], \\ &\dot{\mathbf{m}} = \mathbf{\Omega} \cdot \mathbf{m} + a[\mathbf{D} \cdot \mathbf{m} - \mathbf{D} : \mathbf{mmm}], \end{aligned} \tag{2}$$

where $D_r(\mathbf{m})$ is the rotational diffusivity, k is the Boltzmann constant, T is the absolute temperature, a is the *molecular geometry parameter* which plays an important role in all mesoscopic approximations of Doi kinetic theory,

$$a = \frac{r^2 - 1}{r^2 + 1} \tag{3}$$

$\mathcal{R} = \mathbf{m} \times \frac{\partial}{\partial \mathbf{m}}$ is the rotational gradient operator, and $\frac{D}{Dt}(\bullet)$ denotes the material derivative $\frac{\partial}{\partial t}(\cdot) + \mathbf{v} \cdot \nabla(\cdot)$. In (2), the second moment of $\mathbf{m}$ with respect to the pdf,

$$\mathbf{M} = \langle \mathbf{mm} \rangle = \int_{||\mathbf{m}||=1} \mathbf{mm}\, f(\mathbf{m}, t)\, d\mathbf{m}, \tag{4}$$

enters through the Maier-Saupe excluded-volume potential V,

$$V = -\frac{3}{2} N\, kT\, \mathbf{mm} : \mathbf{M}\,. \tag{5}$$

The mesoscopic *orientation tensor* $\mathbf{Q}$ is the traceless part of $\mathbf{M}$,

$$\mathbf{Q} = \mathbf{M} - \tfrac{1}{3}\,\mathbf{I}, \tag{6}$$

the fundamental mesoscopic variable which links to laboratory measurements [Burghardt (1998), Fuller (1995)]. The nematodynamical equation for $\mathbf{Q}$ is derived from (2):

$$\begin{aligned} \tfrac{d}{dt}\mathbf{Q} \;\; &= \;\; \mathbf{\Omega} \cdot \mathbf{Q} - \mathbf{Q} \cdot \mathbf{\Omega} + a\,[\mathbf{D} \cdot \mathbf{Q} + \mathbf{Q} \cdot \mathbf{D}] + \tfrac{2a}{3}\mathbf{D} - 2a\,\mathbf{D} : \langle \mathbf{mmmm} \rangle \\ &\quad -6\, D_r^0\, [\mathbf{Q} - N\,(\mathbf{Q} + \tfrac{1}{3}\,\mathbf{I}) \cdot \mathbf{Q} + N\,\mathbf{Q} : \langle \mathbf{mmmm} \rangle]\,, \end{aligned} \tag{7}$$

where D_r^0 is an averaged rotary diffusivity [Doi and Edwards (1986)], and the fourth moment tensor $\langle \mathbf{mmmm} \rangle$ enters due to nonlinearities. A huge literature on closure approximations exists (cf., [Chaubal *et al.* (1995)]), leading to mesoscopic models that may be related to the posited mesoscopic theories of Landau-deGennes [de Gennes and Prost (1993)] and Beris-Edwards-Grmela-Ottinger [Beris and Edwards (1994)]. The methods we introduce below can be applied to any mesoscopic $\mathbf{Q}$ tensor model. To make the analysis explicit and to compare with results from alternative methods [Forest and Wang (2002)], we choose the Doi closure which asserts

$$(\bullet) : \langle \mathbf{mmmm} \rangle \approx (\bullet) : \mathbf{MM} \tag{8}$$

for any second-order tensor $(\bullet)$. We also take D_r^0 to be constant to simplify the analysis.

We assume simple shear flow, given in Cartesian coordinates (x, y, z) by

$$\mathbf{v} = \dot{\gamma}\,(y, 0, 0)\,, \tag{9}$$

where $\dot{\gamma}$ is the shear rate. The rate-of-strain and vorticity tensors for (9) are:

$$\mathbf{D} = \dot{\gamma}\,\tilde{\mathbf{D}}, \qquad \mathbf{\Omega} = \dot{\gamma}\,\tilde{\mathbf{\Omega}}\,, \tag{10}$$

$$\tilde{\mathbf{D}} = \frac{1}{2}\begin{pmatrix} 0 & 1 & 0 \\ 1 & 0 & 0 \\ 0 & 0 & 0 \end{pmatrix}, \quad \tilde{\mathbf{\Omega}} = \frac{1}{2}\begin{pmatrix} 0 & 1 & 0 \\ -1 & 0 & 0 \\ 0 & 0 & 0 \end{pmatrix}. \tag{11}$$

The *Peclet number Pe*,

$$Pe = \frac{\dot{\gamma}}{6D_r^0}, \tag{12}$$

is the shear rate normalized relative to nematic relaxation rate, and serves as the basic asymptotic parameter for weak shear.

Finally, recall that $\mathbf{M}$ and $\mathbf{Q}$ share an orthonormal frame of eigenvectors $\mathbf{n}_i$, called *directors*, with corresponding eigenvalues $d_i, i = 1, 2, 3$ of $\mathbf{M}$, $d_i - \frac{1}{3}$ of $\mathbf{Q}$, called the *order parameters.* The director $\mathbf{n}_i$ associated with the *maximum* d_i is the *major director.* Flow-aligned states are classified according to the direction of the major director relative to the shearing (flow(x)-flow gradient(y)) plane: *in-plane* if $\mathbf{n}_i$ lies in the (x,y) plane, and then the polar angle ϕ_L is called the *Leslie alignment angle*; *logrolling* if $\mathbf{n}_i$ is parallel to the vorticity (z) axis; and *out-of-plane* if $\mathbf{n}_i$ lies strictly between the shearing plane and vorticity axis.

3 Weak-shear solvability conditions

All equilibria for the Doi closure model *without flow* admit the uniaxial representation

$$\mathbf{Q_0} = s_{\pm}\,(\mathbf{u}\,\mathbf{u} - \frac{1}{3}\mathbf{I})\,, \tag{13}$$

where $s = 0$ or $\mathbf{Q} = \mathbf{0}$ is the isotropic state that exists for all concentrations, and nematic states exist for sufficiently high $N \geq \frac{8}{3}$ with

$$s_{\pm} = \frac{1}{4}\left(1 \pm 3\sqrt{1 - \frac{8}{3N}}\right)\,, \tag{14}$$

$\mathbf{u}$ is the uniaxial director which is arbitrary in the absence of an applied field; s_+ indicates the upper (stable) nematic branch, s_- labels the lower (unstable) branch.

We uniquely parametrize orientational degeneracy of the nematic phases (13), (14), by a spherical coordinate representation of $\mathbf{u} \in S^2_+$, the half-sphere consisting of the equator (shear plane) union the upper hemisphere:

$$\mathbf{u} = (\sin\theta\cos\phi, \quad \sin\theta\sin\phi, \quad \cos\theta)\,, \qquad \theta \in [0, \frac{\pi}{2}), \quad \phi \in [0, 2\pi]\,. \tag{15}$$

When $\mathbf{u}$ lies in the shear plane $\theta = \frac{\pi}{2}$, uniqueness restricts ϕ to any arc of π radians, which we select as $[-\frac{\pi}{2}, \frac{\pi}{2}]$ following tradition.

In weak shear flows, the goal is to identify those $\mathbf{u}$ which survive as steady states versus N and a, and to identify how this major director perturbs [Kuzuu and Doi (1983, 1984)]. For states which persist from the *nematic* equilibria (13), (14), then the shear-induced steady state $\mathbf{Q}$ will be given by $\mathbf{Q}_0$ at leading order, with an $O(Pe)$ correction to be determined below. To preview our method: *first* we will determine which $\mathbf{u} \in S^2_+$ survive as steady states; *second* we will exactly construct the $O(Pe)$ correction to each shear-selected steady state as an explicit function of the model parameters N and a; and *third*, we will determine stability of each state. Finally, all alignment and rheological properties of stable steady states follow by straightforward evaluation.

In-plane and logrolling shear-alignment are each characterized *either* by the two constraints $Q_{xz} = Q_{yz} = 0$, *or* by assigning one eigenvector of $\mathbf{Q}$ parallel to the vorticity axis. One must then defer to the major director to distinguish them. In our parametrization, $\theta = 0$ corresponds to major director parallel to the vorticity axis; $\theta = \frac{\pi}{2}$ (mod π) yields major director $\mathbf{u}$ in the shear plane; and all other choices of θ yield major director that is out-of-plane. Once special $\mathbf{Q}_0 havebeendeterminedtopersistinweakshear, thentheirmajordirectorgivesaclassification$
$plane, logrolling, orout - of - planeifwecanshowthattheshear - inducedcorrection,$Pe $\mathbf{Q}_1$, maintains that major director alignment. This is part of the method given here.

In general, the shear perturbation is expected to break the director degeneracy *and* the uniaxial order-parameter degeneracy of quiescent equilibria (13), (14); our goal is to determine both selection criteria. We now present the method. Recall the general biaxial representation (see [Forest and Wang (2002)])

$$\begin{aligned}\mathbf{Q} &= \sum_{i=1,2,3} (d_i - \frac{1}{3})\, \mathbf{n}_i \mathbf{n}_i \\ &= s\,(\mathbf{n}_1 \mathbf{n}_1 - \frac{1}{3}\mathbf{I}) + \beta\,(\mathbf{n}_2 \mathbf{n}_2 - \frac{1}{3}\mathbf{I}) \qquad (16)\end{aligned}$$

with $s = d_1 - d_3$, $\beta = d_2 - d_3$. Uniaxial limits are $\beta = 0, s = 0$, or $s = \beta$, where the uniaxial director is $\mathbf{n}_1$, $\mathbf{n}_2$, or $\mathbf{n}_3$, respectively. Biaxial states satisfy $d_i \neq d_j, \forall i, j$, with maximum d_i defining the major director.

Assume weak shear, $Pe \ll 1$, and expand $\mathbf{Q}$ in powers of Pe:

$$\mathbf{Q} = \mathbf{Q}_0 + Pe\,\mathbf{Q}_1 + Pe^2\,\mathbf{Q}_2 + \cdots\,. \qquad (17)$$

At order Pe, for any mesoscopic tensor model, one gets a linearized tensor-operator equation for $\mathbf{Q}_1$:

$$\mathbf{A}(\mathbf{Q}_0) \cdot \mathbf{Q}_1 = \mathbf{r}(\mathbf{Q}_0)\,, \qquad (18)$$

where $\mathbf{A}(\mathbf{Q}_0)$ is the linearized quiescent nematic tensor field, and $\mathbf{r}(\mathbf{Q}_0)$ is the linearized flow perturbation. For the Doi closure model, these operators are given by (with $\mathbf{M}_0 = \mathbf{Q}_0 + \frac{1}{3}\,\mathbf{I}$):

$$\begin{aligned}\mathbf{A}(\mathbf{Q}_0) \cdot \mathbf{Q}_1 &= \mathbf{Q}_1 - N\,(\mathbf{M_0} \cdot \mathbf{Q}_1 + \mathbf{Q}_1 \cdot \mathbf{Q_0}) \\ &\quad + N\,(\mathbf{Q_0} : \mathbf{M_0}\,\mathbf{Q}_1 + \mathbf{Q_1} : \mathbf{M_0} + \mathbf{Q_0} : \mathbf{Q_1})\,\mathbf{M_0} \qquad (19)\\ \mathbf{r}(\mathbf{Q}_0) &= \tilde{\mathbf{\Omega}} \cdot \mathbf{Q_0} - \mathbf{Q_0} \cdot \tilde{\mathbf{\Omega}} + a\left(\tilde{\mathbf{D}} \cdot \mathbf{Q_0} + \mathbf{Q_0} \cdot \tilde{\mathbf{D}}\right) \\ &\quad + a\left(\frac{2}{3}\,\tilde{\mathbf{D}} - 2\,\tilde{\mathbf{D}} : \mathbf{M_0}\,\mathbf{M_0}\right)\,. \qquad (20)\end{aligned}$$

In the analysis deferred to Appendix B, we utilize the Cartesian components of $\mathbf{Q}_1$ to convert the tensor-operator equation (18) to a transparent linear system:

$$A \cdot Q_1 = r\,, \qquad (21)$$

where A is a 5×5 matrix, $Q_1 = (Q_1(xx), Q_1(xy), Q_1(xz), Q_1(yy), Q_1(yz))^T$ comprises the 5 components of $\mathbf{Q}_1$, and r is a 5-vector derived from $\mathbf{r}$, (20).

As in Kuzuu and Doi (1983), the Fredholm alternative theorem provides the weak-shear solvability condition. Those $\mathbf{Q}_0$, defined in (13), (14), uniquely parametrized by $\mathbf{u} \in S^2_+$ from (15), which *remain steady* through $O(Pe)$ are characterized by:

$$r(\mathbf{Q}_0) \perp \mathcal{N}(A^T(\mathbf{Q}_0)), \tag{22}$$

where $\mathcal{N}$ denotes the null space of the matrix A^T. *This solvability condition determines which quiescent states* (13) (14) *persist in weak shear*, including those arising from the stable and unstable nematic equilibrium branches (14), and the isotropic state.

To completely construct $\mathbf{Q}_1$ *for each persistent* $\mathbf{Q}_0$*, to determine stability and out-of-plane transitions versus mesoscopic parameters, we require another order of perturbation.* That is, we need the solvability condition for $\mathbf{Q}_2$. The tensor-equation for $\mathbf{Q}_2$ and corresponding orthogonality condition are given in Appendix A.

4 Steady states in weak shear

We report the physical conclusions from an exact analysis of the solvability conditions for $\mathbf{Q}_1$ and $\mathbf{Q}_2$, equations (22) and (51). We give the *construction* of $\mathbf{Q}_1$ through order $O(Pe)$ for all persistent steady states, first those associated with the quiescent isotropic state, followed by the two nematic branches. We then *deduce directors and order parameters* from the tensor representation (16), and finally display the alignment and rheological properties of all stable steady states. The mathematical analysis is summarized in Appendix B.

4.1 The shear-perturbed, nearly isotropic branch

The isotropic steady state perturbs at $O(Pe)$ to a remarkably simple form,

$$\mathbf{Q} = \mathbf{0} + Pe\,\frac{2\,a}{3-N}\,\tilde{\mathbf{D}} + O(Pe^2)\,, \tag{23}$$

where $\tilde{\mathbf{D}}$ is the normalized rate-of-strain (11) for pure shear. The directors of $\mathbf{Q}$ are explicit,

$$\mathbf{n}_1 = (1,-1,0), \qquad \mathbf{n}_2 = (1,1,0) \qquad \mathbf{n}_3 = (0,0,1)\,, \tag{24}$$

with corresponding distinct order parameters

$$d_1 = \frac{1}{3} + \frac{a}{N-3} Pe, \qquad d_2 = \frac{1}{3} - \frac{a}{N-3} Pe, \qquad d_3 = \frac{1}{3}\,. \tag{25}$$

All features of the shear-perturbed isotropic state follow:

- a *unique* steady state survives for $N \neq 3$;
- it is *biaxial* ($d_i \neq d_j$, if $i \neq j$);
- the major director is always *in-plane*;
- for rods ($a > 0$), the Leslie alignment angle ϕ, to within $O(Pe^2)$, is universal, independent of aspect ratio parameter a and shear rate Pe:
    - 45^o *above* the flow direction when $N < 3$, and
    - 45^o *below* the flow direction when $N > 3$;

  at higher order in Pe, the director tilts toward the flow axis for rods and discotics which we omit; these Doi model results are consistent with kinetic theory as well [Forest *et al.* (2002c)].
- the sign of ϕ, i.e., direction of tilt relative to the flow direction, reverses for discotics ($a < 0$).

From the next order solvability condition, stability is straightforward with explicit linearized eigenvalues

$$\lambda_1 \approx \lambda_2 \approx \lambda_3 \approx \lambda_4 \approx \lambda_5 = -(1 - \frac{N}{3}) + O(Pe)\,. \tag{26}$$

Therefore, *the shear-perturbed isotropic branch is stable for* $N < 3$, and *unstable for* $N > 3$, as expected. We depict the region of stable nearly isotropic states in (a, N) parameter space in Figure 1(b), which summarizes all stable flow aligned states.

We note that this asymptotic construction breaks down for $|N-3| = O(Pe)$, i.e., the solvability equation (22) does not have a solution. This implies *an $O(Pe)$ gap in concentrations $N \approx 3$ where the isotropic branch fails to persist*; this result is indeed confirmed by mesoscopic numerical simulations [Forest and Wang (2002)], and is consistent with kinetic theory [Forest *et al.* (2002b)].

4.2 The stable nematic equilibrium branch

Consider the upper nematic solution $\mathbf{Q}_0$ with order parameter $s_+ \in [\frac{1}{4}, 1)$, (13), (14), which we abbreviate as s in the formulas below. Recall $\mathbf{u} \in S^2_+$, equation (15), gives a 1 : 1 parametrization of rotational symmetry, which we decompose into three disjoint cases defined by *the polar angle θ*: vorticity alignment, shear-plane alignment, and out-of-plane alignment.

4.2.1 Shear perturbed logrolling states: $\theta = 0$

The perturbed solution $\mathbf{Q}$ corresponding to $\mathbf{u} = (0,0,1)$ is explicitly constructed:

$$\mathbf{Q} = \frac{s}{3}\begin{pmatrix} 1 & 0 & 0 \\ 0 & 1 & 0 \\ 0 & 0 & -2 \end{pmatrix} + Pe\frac{a(1-s)^2(1+2s)}{9\,s}\begin{pmatrix} 0 & 1 & 0 \\ 1 & 0 & 0 \\ 0 & 0 & 0 \end{pmatrix} + O(Pe^2)\,, \tag{27}$$

with *distinct* order parameters at $O(Pe)$:

$$d_1 = \frac{2s+1}{3}, \tag{28}$$

$$d_2 = \frac{1-s}{3} - a\,Pe\,\frac{1-3s^2+2s^3}{3s}, \tag{29}$$

$$d_3 = \frac{1-s}{3} + a\,Pe\,\frac{1-3s^2+2s^3}{3s}, \tag{30}$$

and corresponding directors

$$\mathbf{n}_1 = (0,0,1), \quad \mathbf{n}_2 = (1,-1,0), \quad \mathbf{n}_3 = (1,1,0), \tag{31}$$

respectively. *All features of the logrolling equilibrium in weak shear follow*:

- the logrolling equilibrium *always exists*, for all nematic concentrations $N > \frac{8}{3}$ and all aspect ratios;

- the major director remains aligned with the vorticity axis, i.e., *the shear-selected equilibrium is logrolling through $O(Pe)$*;

- the equilibrium is *biaxial*, $d_i \neq d_j$ for $i \neq j$, with maximum degree of order $d_1 = \frac{2s+1}{3}$ that remains constant to $O(Pe)$;

- the minor directors are *universal*, similar to the isotropic state, in the sense that they are aligned at 45^o in the shear plane independent of concentration N and shape parameter a. These properties follow because $\mathbf{Q}_1$ is proportional to the rate-of-strain tensor $\tilde{\mathbf{D}}$, from (27).

This recovers the result from [Forest and Wang (2002)], by a completely different method, that *the Doi closure preserves vorticity-aligning steady states for all aspect ratios and nematic concentrations.* The method of this paper also shows (private notes) the Hinch-Leal closures [Hinch and Leal (1972)] agree with the Doi closure in unconditional preservation of logrolling equilibria, whereas the Tsuji-Rey closure [Tsuji and Rey (1997)] has one isolated concentration, independent of a, where the logrolling equilibrium does not exist. Closures are extremely sensitive with respect to stability of shear-selected equilibria, as reported from numerical simulations in [Forest and Wang (2002)], which we now determine.

The logrolling state is unstable for the Doi closure. This analysis is delicate, requiring separate treatment of the in-plane tensor subspace (where logrolling states are stable) and the two linearized eigenvalues corresponding to *out-of-plane* degrees of freedom. Indeed, the out-of-plane eigenvalues (which describe potential "director tipping instabilities") are $O(Pe^2)$, whose evaluation requires explicit construction of $\mathbf{Q}_2$ as well as $\mathbf{Q}_1$. The pair of out-of-plane eigenvalues of the linearized system, to $O(Pe^2)$, are

$$Pe\,\frac{2a^2\,Pe\,(1+s-2s^2)^2 \pm 9s\sqrt{-9s^2+a^2(2+s)^2}}{54s^2}. \tag{32}$$

For s not near 1 (N finite), one of these two eigenvalues must be positive or have positive real part. Therefore, *the logrolling solution is unconditionally unstable.* When s is near

1, i.e., $N \gg 1$, the real parts of these two eigenvalues (for $|a| \neq 1$) approach zero. This result suggests a stability transition for logrolling equilibria of finite-aspect-ratio liquids in the high concentration limit. Indeed, numerically the Doi closure model is found to undergo a supercritical Hopf bifurcation for $N \gg 1$ and all $|a| < 1$ at which the logrolling equilibrium stabilizes at the same critical concentration at which the stable kayaking state destabilizes; we refer to [Forest *et al.* (2002d)].

4.2.2 Shear perturbed in-plane flow-aligned states: $\theta = \frac{\pi}{2}$

An in-plane major director (15) reduces to $\mathbf{u}_0 = (\cos\phi, \sin\phi, 0)$ for some angle ϕ. Analysis of the solvability conditions shows that *flow-alignment requires sufficiently extreme molecule aspect ratios* r **and** *nematic, but not too high, concentrations* N:

- for $\frac{1}{\sqrt{2}} < r < \sqrt{2}$, i.e., $|a| < \frac{1}{3}$, in-plane flow-alignment does *not* occur;
- if $\sqrt{2} < r < \infty$ or $0 < r < \frac{1}{\sqrt{2}}$, i.e., $\frac{1}{3} < |a| < 1$, flow-aligned steady states exist for a finite range of nematic concentrations, $\dfrac{8}{3} < N \leq \dfrac{(3-|a|)^2}{3(1-a^2)}$; when these conditions are met, our construction gives the Leslie alignment angle ϕ_L
$$\cos 2\phi_L = \frac{3\,s}{a\,(s+2)} = \frac{1 + 3\sqrt{1-\frac{8}{3N}}}{a\,(3+\sqrt{1-\frac{8}{3N}})}\,, \tag{33}$$
which is equivalent to the formulas derived by Cocchini *et al.* (1990), Wang (1997), Rienacker and Hess (1999), Maffettone *et al.* (2000), Forest and Wang (2002), and Grecov and Rey (2002) by different methods.
- If $r = 0$ or $r = \infty$, i.e., $|a| = 1$, the flow aligned state always exists for any $N > \dfrac{8}{3}$, with Leslie alignment angle (33).
- If $r = \sqrt{2}$ or $r = \frac{1}{\sqrt{2}}$, i.e., $|a| = \frac{1}{3}$, flow-alignment only exists at $N = \frac{8}{3}$, with $\phi = 0$ for $a = \frac{1}{3}$, $\phi = \frac{\pi}{2}$ for $a = -\frac{1}{3}$.

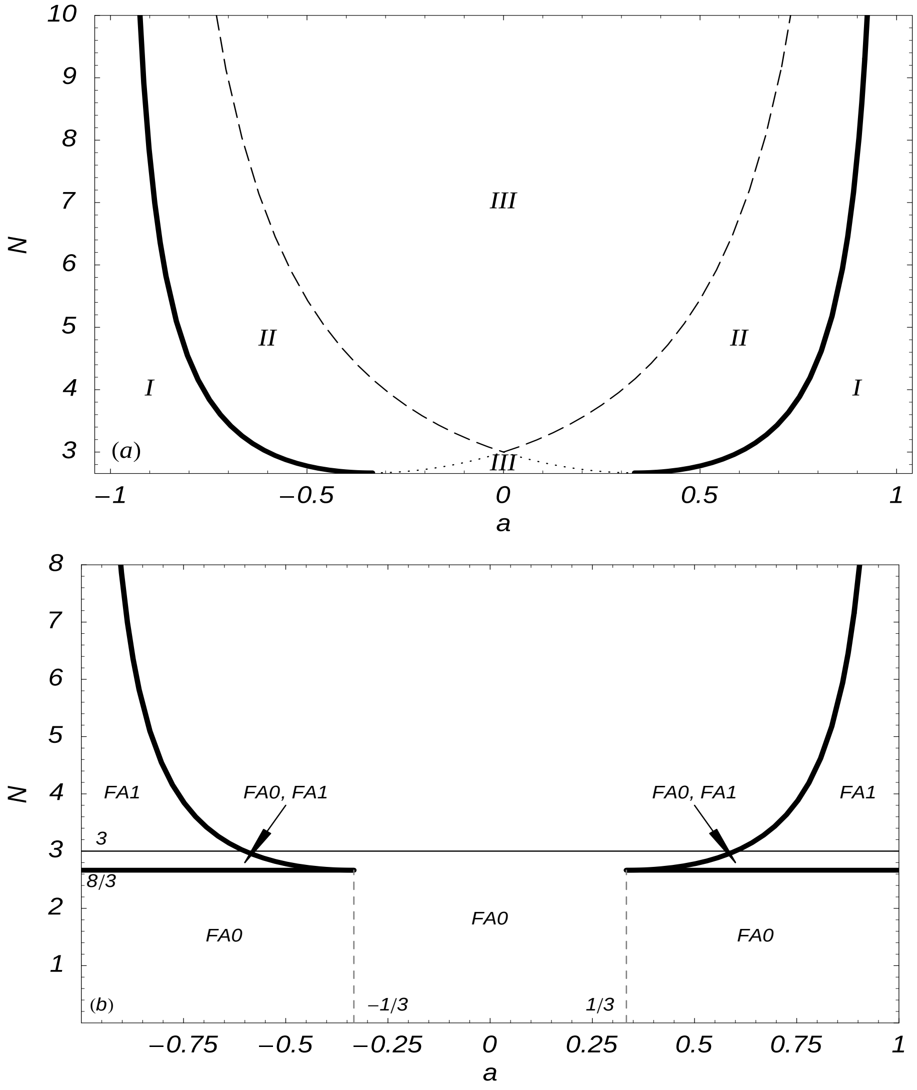

Figure 1: **(a)**: Regions in (a, N) space of shear-aligned *nematic* steady states. See Table 1 for specific types of steady states for each region. The solid boundary between region (I) and (II) corresponds both to loss of the stable flow-aligning state and existence of the out-of-plane state. **(b)**: Regions of *all stable* steady states, both nearly isotropic (**FA0**) and nematic (**FA1**).

In regimes where the flow-alignment states exist, the perturbed solution $\mathbf{Q}$ is explicitly constructed to $O(Pe)$ as

$$\mathbf{Q} = s\,(\mathbf{u}_0\mathbf{u}_0 - \frac{\mathbf{I}}{3}) + Pe\left[c_1\,\tilde{\mathbf{D}} + c_2\begin{pmatrix} 1 & 0 & 0 \\ 0 & 1 & 0 \\ 0 & 0 & -2 \end{pmatrix} + c_3\begin{pmatrix} 1 & 0 & 0 \\ 0 & -1 & 0 \\ 0 & 0 & 0 \end{pmatrix}\right] + O(Pe^2), \qquad (34)$$

where s is fixed by N, equation (14), $\mathbf{u}_0$ is given above, $\phi = \phi_L$ is given by (33), and

$$\begin{aligned} c_1 &= \frac{(1-s)^2(1+2s)}{18s(4s-1)}\left(11s + 4 - \frac{9s^2(19s+8)}{a(2+s)^2}\right), \\ c_2 &= \frac{(1-s)^2(1+2s)\tan 2\phi}{6\,(4s-1)}, \\ c_3 &= \frac{3s(1-s)^2(1+2s)(19s+8)\tan 2\phi}{6\,a\,(2+s)^2(4s-1)}. \end{aligned}$$

Transition behavior of in-plane flow-aligned states can be deduced from equation (33). In fact, equation (33) provides an explicit relationship between the critical concentration N_* and the aspect ratio parameter a, where flow-aligned in-plane states fail to persist:

$$N_*(a) = \frac{(3-|a|)^2}{3(1-a^2)}. \qquad (35)$$

This boundary is the solid curve in Figure 1(a), which separates the parameter space (a, N) of the Doi closure model into regions where various flow-aligned states exist or not. Boundaries for other steady states arising from nematic equilibria are also given. Figure 1(a) and Table 1 therefore display all persistent (stable and unstable) steady states in the weak shear limit for all mesoscopic parameters (a, N).

To illustrate the information contained in Region (I) in Figure 1(a), consider three distinct aspect ratios corresponding to $a = 0.7, 0.8, 0.9$. Our theory predicts flow-aligned stable nematic states exist for $\frac{8}{3} < N < \frac{529}{153}$, $\frac{8}{3} < N < \frac{121}{27}$, $\frac{8}{3} < N < \frac{147}{19}$, respectively, whose explicit Leslie alignment angle is graphed in Figure 2. We also show the alignment angle ϕ_L for three distinct nematic concentrations $N = 3, 4, 10$, which reveals the scaling behavior of in-plane alignment versus molecular aspect ratio, and the limiting behavior as these states cease to exist. This region in Figure 1(a), as shown, has five other steady nematic states, all unstable, as well as a nearly isotropic unstable state.

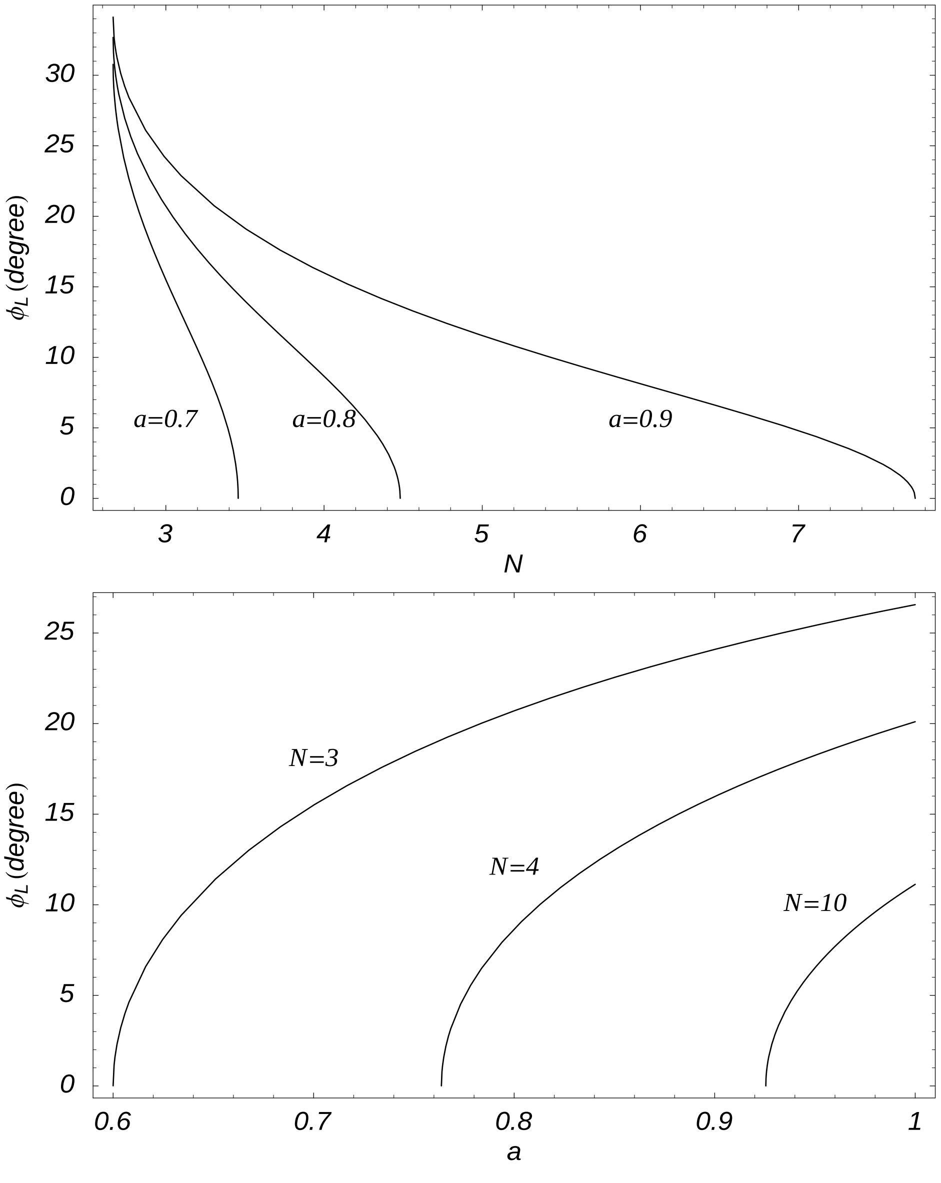

Figure 2: Explicit alignment properties of stable in-plane states from Region I, Figure 1a. Top: The Leslie alignment angle ϕ_L for solutions along three vertical slices of Figure 1a corresponding to aspect ratio parameters $a = 0.7, 0.8, 0.9$. Bottom: ϕ_L for three horizontal slices of Figure 1a, $N = 3, 4, 10$.

I	**FA0**, $\mathbf{FA}_{+}^{1,2}$, $\mathbf{FA}_{-}^{1,2}$, $\mathbf{LR}_{\pm}$
II	**FA0**, $\mathbf{FA}_{-}^{1,2}$, $\mathbf{LR}_{\pm}$
III	**FA0**, $\mathbf{LR}_{\pm}$
Solid curve	**FA0**, $\mathbf{OS}_{+}^{1,2}$
Dashed curve	**FA0**, $\mathbf{OS}_{-}^{1,2}$
Dotted curve	**FA0**, $\mathbf{OS}_{-}^{3,4}$

Table 1: Shear-selected steady states in weak shear for each region in (a, N) space. **FA0** is the only flow-aligning steady state selected from the isotropic branch. Others are selected from nematic branch. **FA** indicates flow-aligning state, **LR** logrolling state, **OS** out-of-plane steady state. "+" indicates surviving from the upper nematic branch, "$-$" the lower nematic branch. "1", "2" label multiplicity. For example, six steady nematic states and a nearly isotropic steady state exists in region (I).

We note that this critical nematic concentration (N_*) for each extreme aspect ratio, equation (35), varies with closure approximations. However, *the existence of a cut-off condition* like (35) *is robust* to closure as determined from different methods in [Forest and Wang (2002)]. From Figure 2, one concludes certain robust features:

- at the clearing point of quiescent nematics, $N = \frac{8}{3}$, in-plane shear-aligned states begin with Leslie angle $\phi_L = \frac{1}{2}Cos^{-1}(\frac{1}{3a})$, which is nearly constant across a huge aspect ratio range;
- the range of concentrations over which stable in-plane alignment persists is strongly dependent on the aspect ratio parameter a, with explicit scaling law given above;
- all shear-aligned states terminate at a critical concentration with zero Leslie angle, $\phi_L = 0$, which we shall soon show coincides with an out-of-plane steady transition!

When the alignment condition (33) is satisfied, i.e., below the solid curves in Figure 1, two in-plane Leslie alignment angles, $\phi_{\pm}$ with opposite signs, are selected at the onset of shear from (33). The linearized eigenvalues of the dynamical system (7), (8) are given by

$$\lambda_1 = -\frac{3\,s}{(1-s)(1+2s)} + O(Pe)\,, \tag{36}$$

$$\lambda_2 = -Pe\,\frac{a\,(2+s)(1+5s)}{6\,s(4s-1)}\,\sin 2\phi + O(Pe^2)\,, \tag{37}$$

$$\lambda_3 = -\frac{3\,s}{(1-s)(1+2s)} + O(Pe)\,, \tag{38}$$

$$\lambda_4 = -\frac{s(4s-1)}{(1-s)(1+2s)} + O(Pe)\,, \tag{39}$$

$$\lambda_5 = -Pe\,\frac{a\,(2+s)}{3\,s}\,\sin 2\phi + O(Pe^2)\,, \tag{40}$$

The $O(Pe)$ eigenvalues λ_2 and λ_5 characterize the shear-broken zero eigenvalues of orientational degeneracy. *If* $a \sin 2\phi > 0$*, then all 5 eigenvalues are negative and the solution is stable.* The other in-plane solution is then unstable, with λ_2, $\lambda_5 > 0$. We conclude: *for rods*, if the steady state has positive Leslie alignment angle, then it is stable, otherwise, it is unstable; *for discotics*, if the steady state has negative Leslie alignment angle, then it is stable, otherwise, it is unstable. The rod-discotic correspondence is also a consequence of a symmetry, derived in [Forest and Wang (2002)] for mesoscopic theory and in [Forest *et al.* (2002a)] for kinetic theory.

Finally, the angle in (33) gives the quiescent director that will survive at first order in perturbation. The shear-perturbed correction can be found explicitly:

$$\cos 2\tilde{\phi} = \cos 2\phi - Pe\,\frac{(1-s)^2(1+2s)(4+11s)\sin 2\phi}{3\,s\,(2+s)(4s-1)} + O(Pe^2)\,. \tag{41}$$

This exact formula shows *the Leslie alignment angle always increases* ($\tilde{\phi} \geq \phi$) *with shear rate*, i.e., the major director of the in-plane nematic steady state always moves counterclockwise with increased shear rate for any shape parameter a. This is a feature precisely in the L-E limit of Doi theory, relying only on uniaxial properties of the quiescent nematic and only applicable in the weak shear limit. However, this behavior is beyond L-E theory, which predicts the Leslie alignment angle is independent of shear rate. We illustrate the weak shear dependence of the Leslie alignment angle for a fixed nematic concentration $N = 6$ and a fixed, large aspect ratio $a = .95$, in Figure **??**$\text{vs}_{Pe}\phi_v s_{Pe}$

RUHAI: we should choose a fixed N=6, and fixed a=.95, and give the low Pe variation in the Leslie alignment angle for .01 to .10.

4.2.3 Out-of-plane flow-aligned states: $0 < \theta < \frac{\pi}{2}$

Analysis (outlined in the Appendix) of the solvability conditions shows *pairs of out-of-plane solutions*, mirror-symmetric with respect to the shearing plane, are indeed *selected in the weak shear limit*, but *only under two conditions*:

- the aspect ratio must be sufficiently extreme, but finite: $\frac{1}{3} \leq |a| < 1$;
- the concentration must be a unique finite value,

$$N = \frac{(3 - |a|)^2}{3(1 - a^2)}\,. \tag{42}$$

Comparison of (35), (42) shows *out-of-plane steady states exist precisely where the in-plane flow-aligning states disappear with Leslie angle* $\phi = 0$, and thereby serve an intriguing role to deliver the stable flow-aligning state out of the shearing plane. (This analytical result of the Doi closure agrees, to within $O(Pe)$, with kinetic simulations [Forest *et al.* (2002b)].)

The analysis here confirms another symmetry discussed in [Faraoni *et al.* (1999), Forest *et al.* (2002a), Forest and Wang (2002)], mirror-reflection about the shear plane. Notice that (θ, ϕ) and $(\pi - \theta, \pi + \phi)$ (which have opposite direction) correspond to the same director. Take $\frac{1}{3} \leq a < 1$ for example: two out-of-plane solutions (for a specific θ) survive when $\phi = 0$ and $\phi = \pi$. $(\theta, 0)$ and (θ, π) (equivalent to $(\pi - \theta, 0)$) are in fact symmetric about the shear plane ($\theta = \frac{\pi}{2}$). If we vary θ, we would get a half circle of directors in the x-z plane that connects to the logrolling state ($\theta = 0$) and the flow-aligning state ($\theta = \frac{\pi}{2}$). This half circle of directors corresponds to the vertical lines shown in Figures 5, 6 for small Pe. As Pe becomes larger, this vertical line evolves to a circle, see, e.g., [Faraoni *et al.* (1999), Chillingworth *et al.* (2001), Forest *et al.* (2002b)].

4.3 Lower nematic solution branch

The same analysis outlined above can be applied to the lower quiescent nematic branch, s_- in (14). Since these equilibria are all unstable at rest, they remain unstable in the weak shear limit. Only at higher shear rates can unstable-stable transitions occur, which does happen but that is not the focus of this paper. Their analysis is necessary for our stated purpose to give a complete accounting of all stable and unstable stationary distributions that survive in weak shear. For the Doi closure, the unstable nematic equilibrium branch breaks orientational degeneracy in a similar manner as the upper stable equilibrium nematic phase. The logrolling state always persists, the flow-aligning states exist below a precise boundary

$$N_-(a) = \frac{(3+|a|)^2}{3(1-a^2)} \tag{43}$$

for $|a| \geq \frac{1}{3}$, and between $N_-(a)$ and $N_*(a)$ for $|a| < \frac{1}{3}$, and the out-of-plane steady transition occurs precisely at these two boundaries. The differences are quantitative, with the results given in Figure 1(a).

The essential difference between this result and that for the upper nematic branch is that here flow-aligned states exist for *all* aspect ratios, consistent with results in [Forest and Wang (2002)].

5 Rheological properties of stable steady states

The stable, robust steady states that have been characterized in detail by our analysis consist of the nearly isotropic, flow-aligned solutions in the dilute concentration regime, labelled **FA0**, Figure 1b, and the in-plane, flow-aligned nematic solutions in the intermediate concentration regime, labelled **FA1**, Figure 1b. (The out-of-plane flow-aligned states are rare, and not likely to be experimentally observed.) The rheological properties of these

-bb-error = =

Figure 3: First and second normal stress differences N_1 and N_2, and the apparent viscosity η versus nematic concentration N for the stable, nearly isotropic, flow aligned states **FA0** of Figure 1b. The parameters chosen are $a = 0.8$, or aspect ratio $r = 3$, and normalized shear rate $Pe = 0.1$.

-bb-error = =

Figure 4: First and second normal stress differences and apparent viscosity for the stable, in-plane, shear-aligned state **FA1**, Figure 1b, selected from the stable quiescent nematic solution, for all nematic concentrations $N > \frac{8}{3}$. The molecular aspect ratio is $r = 3$, and the normalized shear rate is $Pe = 0.1$.

robust attracting states follow directly from the explicit formulas for $\mathbf{Q} = \mathbf{Q}_0 + Pe\,\mathbf{Q}_1$, given above. For the Doi theory, the stress tensor is given by Wang (2002):

$$\begin{aligned} \tau = {} & (\tfrac{2}{Re} + 3\nu kT\zeta_3(a))\mathbf{D} + 3a\nu kT[\mathbf{Q} - N(\mathbf{Q} + \tfrac{\mathbf{I}}{3})\mathbf{Q} + N\mathbf{Q} : \langle\mathbf{mmmm}\rangle] \\ & + 3\nu kT[\zeta_1(a)(\mathbf{DM} + \mathbf{MD}) + \zeta_2(a)\mathbf{D} : \langle\mathbf{mmmm}\rangle], \end{aligned} \tag{44}$$

where

$$\begin{aligned} & \zeta_3 = \tfrac{\zeta^{(0)}}{I_1}, \quad \zeta_1 = \zeta^{(0)}(\tfrac{1}{I_3} - \tfrac{1}{I_1}), \quad \zeta_2 = \zeta^{(0)}[\tfrac{J_1}{I_1 J_3} + \tfrac{1}{I_1} - \tfrac{2}{I_3}], \\ & r = \sqrt{\tfrac{1+a}{1-a}}, \quad I_1 = 2r\int_0^\infty \tfrac{dx}{\sqrt{(r^2+x)(1+x)^3}}, \\ & I_3 = r(r^2+1)\int_0^\infty \tfrac{dx}{\sqrt{(r^2+x)(1+x)^2(r^2+x)}}, \\ & J_1 = r\int_0^\infty \tfrac{x\,dx}{\sqrt{(r^2+x)(1+x)^3}}, \quad J_3 = r\int_0^\infty \tfrac{x\,dx}{\sqrt{(r^2+x)(1+x)^2(r^2+x)}}\,, \end{aligned} \tag{45}$$

and ν is the number density of LCP molecules per unit volume. The apparent viscosity η, first and second normal stress differences N_1 and N_2, are given by

$$N_1 = \tau_{xx} - \tau_{yy}\,, \tag{46}$$

$$N_2 = \tau_{yy} - \tau_{zz}\,, \tag{47}$$

$$\eta = \tau_{xy}/Pe\,. \tag{48}$$

After scaling by $3\nu kT$, these rheological properties are depicted in Figure 3 and Figure 4, where we have chosen $a = 0.8$ ($r = 3$) and $Pe = 0.1$. For η, the viscous contribution is assumed negligible.

In the *dilute concentration regime*, where the nearly isotropic, flow-aligned state is the unique attractor: $N_1 = 0$; N_2 is small but increasingly negative as N increases; the apparent viscosity is constant for very low N then shear hardens as the instability transition is approached. We are not aware of experimental data to benchmark this prediction.

At *nematic concentrations*, in the flow-aligned region of N, a:

- $N_1 > 0$ and $N_2 < 0$, which is consistent with experimental data for flow-aligned nematic polymers in weak shear (cf., [Moldenaers and Mewis (1993), Burghardt (1998), Larson (1998)]).

- The scaling behavior of the first and second normal stress differences versus nematic concentration N, for a fixed aspect ratio and shear rate, is conveyed by Figure 4(a).
- Both N_1 and N_2 approach 0 at the critical concentration $N_*(a)$, i.e., at the transition from stable in-plane alignment to unsteady response! This result suggests a sign change in N_1 and N_2, or even oscillations in their sign, as the unsteady (kayaking) state emerges at slightly higher concentrations.
- The standard rheological data on sign changes in N_1, N_2 correspond to shear-rate transitions. This result implies sign changes in normal stress differences are also associated with concentration-induced, steady-unsteady transitions at very low shear rates.
- RUHAI: is it also the case that if we fix N and vary a that N_1, N_2 change sign?
- FILL IN THE ANSWER TO THIS QUESTION, not necessarily a graph
- The apparent viscosity exhibits *shear thinning* over this range of concentrations. The orientational viscosity is low as the steady-unsteady transition is approached; this prediction is reasonable given the tendency illustrated in Figure 2 for the Leslie alignment angle to approach the flow axis as N approaches the unsteady transition.

6 Numerical confirmation

We use two examples to confirm the results in Figure 1, corresponding to vertical slices at two fixed rod-like aspect ratios. First, we take $r = 3$, or $a = \frac{4}{5} > \frac{1}{3}$, a relatively large aspect ratio, and compute all steady solutions of the full Doi closure model versus nematic concentration N, at fixed weak shear rate

RUHAI: we need to clean this up: gamma dot is DIMENSIONAL, so we have to correct how this is stated here and in the captions.

$De = 0.01$, where $De = 6Pe$. We then choose a less extreme, nearly spherical, aspect ratio $r = \sqrt{\frac{3}{2}}$, or $a = \frac{1}{5} < \frac{1}{3}$. The bifurcation diagrams of four components of the numerical

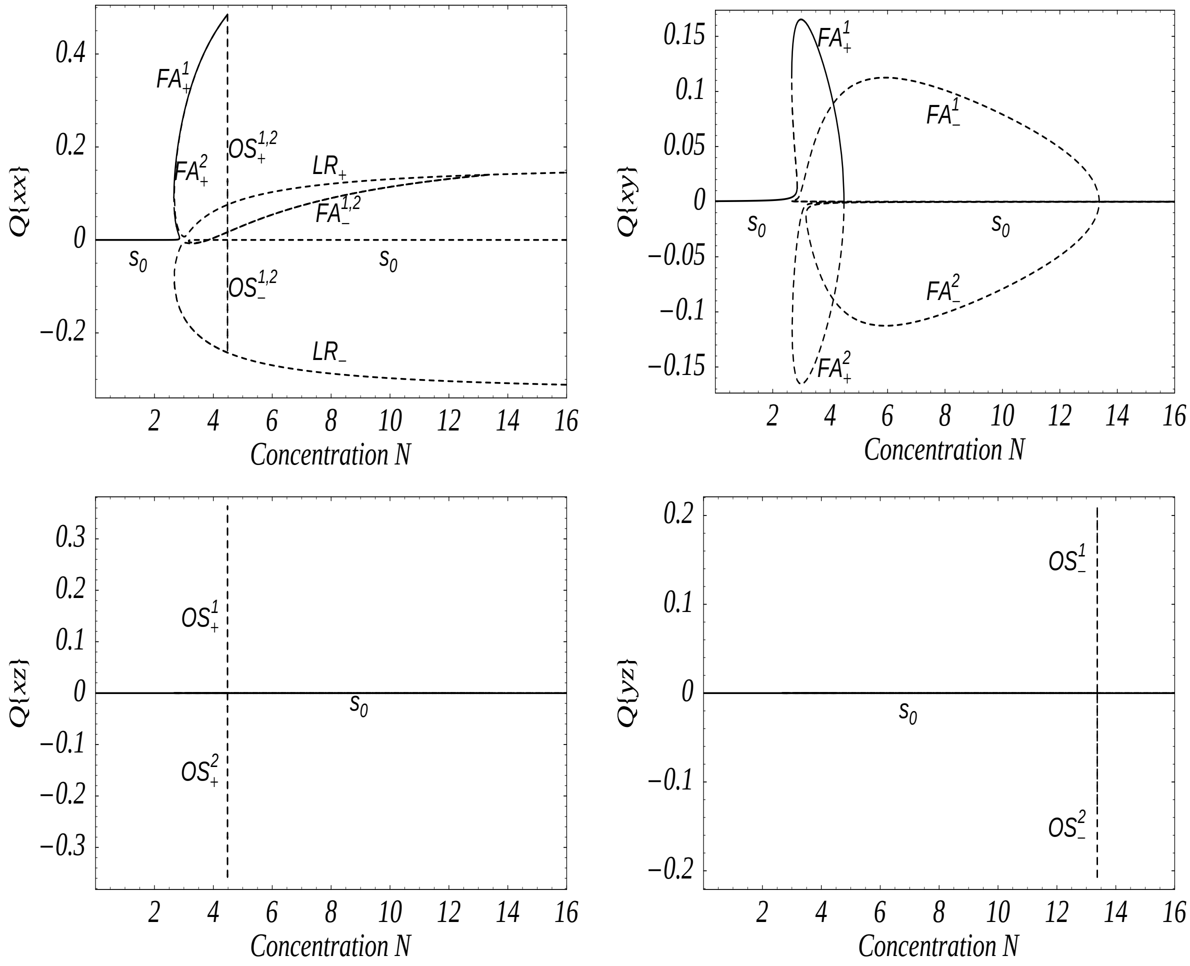

Figure 5: Numerical bifurcation diagram of steady solutions for the Doi closure model with aspect ratio $r = 3$ ($a = \frac{4}{5}$), and weak normalized shear rate $De = 0.01$, where the Deborah number $De = 6Pe$. Solutions are depicted versus nematic concentration N. Out-of-plane solutions emerge at $N = 4.481482$ and 13.37037, which is to be compared with the theoretical predictions of $N = \frac{121}{27} \approx 4.481481$ and $N = \frac{361}{27} \approx 13.37037$. Agreement is within $O(Pe^2)$, as the method predicts. Note that in-plane states are identified by zero out-of-plane components, $Q(xz) = Q(yz) = 0$. The solid line represents the only stable branch.

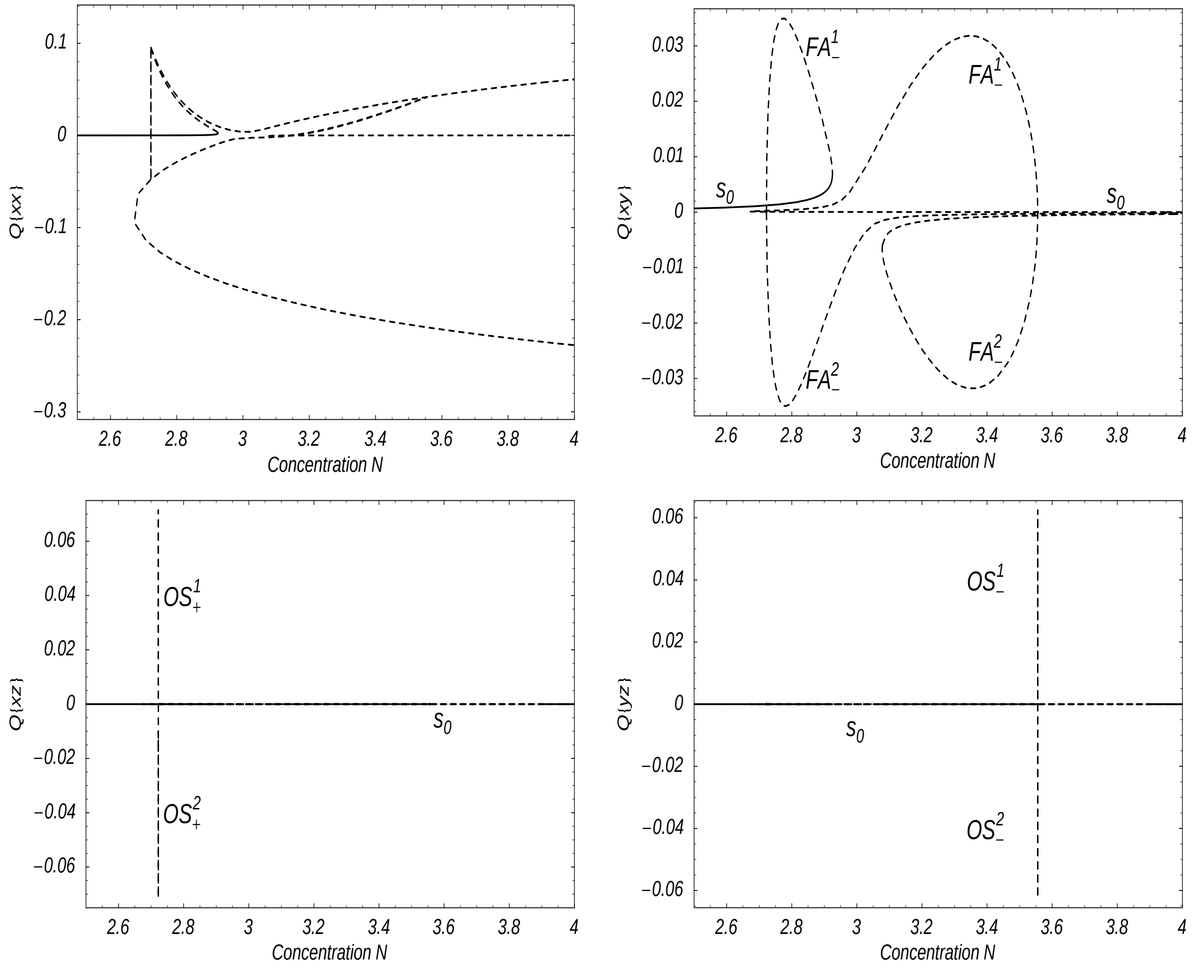

Figure 6: Numerical bifurcation diagram of the Doi closure model for nearly spherical aspect ratio $r = \sqrt{\frac{3}{2}}$ ($a = \frac{1}{5}$), and weak normalized shear rate $De = 0.01$. The out-of-plane solutions emerge at $N = 2.722229$ and 3.555548, whereas our theory predicts $N = \frac{49}{38}$ and $N = \frac{32}{9}$, which agree to well within $O(Pe^2)$.

solutions are shown in Figure 5 and Figure 6. For both examples, the termination of the in-plane solution and the emergence of the out-of-plane solution are predicted with an error within order $O(Pe^2)$. Typically, the flow-aligning solutions exist from the smallest value of $N = \frac{8}{3}$ for $a = \frac{4}{5}$, and terminate at the predicted value at $N = \frac{121}{27}$ for the upper branch and at $N = \frac{361}{27}$ for the lower branch. For $a = \frac{1}{5}$, the flow-aligning solution exists only between two values of N where out-of-plane solutions emerge, predicted by our theory at $N = \frac{49}{38}$ and $N = \frac{32}{9}$.

7 Conclusion

Weak-shear solvability criteria have been derived for general mesoscopic tensor models, giving an analog of the Kuzuu-Doi kinetic theory method. These tensor conditions characterize *all* steady solutions which survive in the weak shear limit from the quiescent equilibrium set. For the special case of the Doi closure, we provide a complete analysis of the solvability conditions, and carry the analysis to sufficient order to construct each steady solution and determine their stability. The number, type, stability, and phase transitions of steady orientational distributions varies with nematic concentration N and molecular aspect ratio r, as detailed in the body. The number of steady states varies between 3 and 7 for the Doi closure; the subset of *stable steady states* is between 0 and 2, either in-plane flow-aligned or out-of-plane aligned states, and possibly a stable logrolling state only at extremely high concentrations $N \gg 1$ and finite aspect ratios. The method is general, and can be applied to any mesoscopic tensor model; the requisite analysis consists of solving five-dimensional linear systems in closed form, which is achievable for the Doi closure model. Our analysis is in complete agreement, qualitatively and quantitatively, with numerical flow-phase diagrams, so that there is no question as to the number, type, and stability of steady states that are selected in weak shear for the Doi closure model. Furthermore, the explicit formulas derived for all robust stable alignment states infer measurable properties (alignment angle, birefringence, first and second normal stress differences, apparent viscosity) and their scaling behavior with respect to nematic concentration and molecular aspect ratio, which are much harder to generate in the laboratory than shear-rate scaling properties.

References

[1] Beris, A.N., Edwards, B.J., **Thermodynamics of Flowing Systems with Internal Microstructure**, Oxford Science Publications (1994).

[2] Burghardt, W.R., Macromol. Chem. Phys. **199**, 471-488 (1998).

[3] Chaubal, C.V., Leal, L.G., Fredrickson, G.H., J. Rheol. **39**, 73-103 (1995).

[4] Chillingworth, D.R.J., Vicente Alonso, E., Wheeler, A.A., J. Phys. A **34**, 1393-1404 (2001).

[5] Cocchini, F, Aratar, C., Marrucci, G., Macromolecules **23**, 4446-4451 (1990)

[6] de Gennes, P.-G., Prost, J., **The Physics of Liquid Crystals**, Oxford University Press (1993).

[7] Doi, M., J. Polym. Sci., Polym. Phys. Ed. **19**, 229-243 (1981).

[8] Doi, M. and Edwards, S. F., **The Theory of Polymer Dynamics**, Oxford U. Press (Clarendon), London-New York (1986).

[9] Faraoni, V., Grosso, M., Crescitelli, S., Maffettone, P. L., J. Rheol. **43**, 829-843 (1999).

[10] Feng, J., Sgalari, G., Leal, G., J. Rheol. **45** (5), 1085-1101 (2000).

[11] Forest, M. G., Wang, Q., Zhou, H., Phys. Fluids **12**(3), 490-498 (2000).

[12] Forest, M.G., Wang, Q., Rheol. Acta, to appear (2002).

[13] Forest, M.G., Wang, Q., Zhou, R., Physical Review E, to appear (2002a).

[14] Forest, M.G., Wang, Q., Zhou, R., The weak shear phase diagram for nematic polymers, UNC Program in Applied Mathematics Preprint No. PAMPS2002-16 (2002b), submitted to Rheologica Acta.

[15] Forest, M.G., Wang, Q., Zhou, R., UNC Program in Applied Mathematics Preprint No. PAMPS2002-26 (2002c), submitted to ASME Proceedings of November, 2002, Annual Meeting.

[16] Forest, M.G., Wang, Q., Zhou, H., Structure evolution in tumbling and kayaking nematic LCPs between shearing plates, UNC Program in Applied Mathematics Preprint No. PAMPS2002-2 (2002d).

[17] Fuller, G.G., **Optical Rheometry of Complex Fluids**, Oxford University Press, Oxford (1995).

[18] Grecov, D., Rey, A., Molec. Cryst. Liquid Cryst., to appear (2002).

[19] Hess, S., Z. Naturforsch Teil **31A**, 1034 (1976).

[20] Hinch, E.J., and Leal, L.G., J. Fluid Mech. **52**(4), 683-712 (1972).

[21] Kuzuu, N., Doi, M.J., Phys. Soc. Japan **52**, 3486-3494 (1983).

[22] Kuzuu, N., Doi, M. J., Phys. Soc. Japan **53**, 1031-1040 (1984).

[23] Landau, L.D., In *Collected papers* (ed. S. Kranse), p.193, Gordon and Breach, New York (1965).

[24] Larson, R.G., Macromolecules **23**, 3983-3992 (1990).

[25] Larson, R.G., **Rheology of Complex Fluids**, Oxford University Press (1998).

[26] Larson, R.G., Ottinger, H., Macromolecules **24**, 6270-6282 (1991).

[27] Maffettone, P.L., Sonnet, A.M., Virga, E.G., J. Non-Newt. Fluid Mech. **90**, 283-297 (2000).

[28] Marrucci, G., Grizzuti, N., paper presented at the 59th Annual Meeting of the Society of Rheology, Atlanta, Ga, October (1987).

[29] Marrucci, G., Macromolecules **24**, 4176-4182 (1991).

[30] Marrucci, G., Greco, F., Mol. Cryst. Liq. Cryst. **206**, 17-30 (1991).

[31] Marrucci, G., Greco, F., Adv. Chem. Phys. **86**, 331-404 (1993).

[32] Marrucci, G., Maffettone, P.L., Macromolecules **22**, 4076-4082 (1989).

[33] Mather, P.T., Pearson, D.S., Larson, R.G., Liquid Crystals **20**(5), 527-538 (1996).

[34] Mather, P.T., Pearson, D.S., Larson, R.G., Liquid Crystals **20**(5), 539-546 (1996).

[35] Mewis, J., Mortier, M., Vermant, J., Moldenaers, P., Macromolecules, **30**, 1323-1328 (1997).

[36] Moldenaers, P., Mewis, J., J. Rheol. **37**(2), 367-380 (1993).

[37] Rienacker, G., Hess, S., Physica A **267**, 294-321 (1999).

[38] Tsuji, T. Rey, A.D., J. Non-Newt. Fluid Mech. **73**, 127-152 (1997)

[39] Ugaz, V.M., Burghardt, R., Zhou, W., Kornfield, J.A., **45** (5), 1029-1062 (2001).

[40] Van Horn, B.L., Winter, H.H., Rheol. Acta **39**, 294-300 (2000).

[41] Wang, Q., J. Rheol. **41**(5), 943-970 (1997).

[42] Wang, Q., J. Chem Phys. **116**(20), 9120-9136 (2002).

[43] Zhou, W.J., Kornfield, J., Burghardt, W., Macromolecules, **34**, 3654-3660 (2001).

A Solvability condition for $\mathbf{Q}_2$

The tensor equation for $\mathbf{Q}_2$ is:

$$\overline{\mathbf{A}}(\mathbf{Q_0},\mathbf{Q_1})\cdot\mathbf{Q_2}=\overline{\mathbf{r}}(\mathbf{Q}_0,\mathbf{Q}_1)\,, \tag{49}$$

where,

$$\begin{aligned}
\overline{\mathbf{A}}(\mathbf{Q}_0,\mathbf{Q}_1)\cdot\mathbf{Q}_2 &= \mathbf{Q}_2-N\,\left(\mathbf{M_0}\cdot\mathbf{Q}_2+\mathbf{Q}_2\cdot\mathbf{Q_0}\right)\\
&\quad +N\left(\mathbf{Q_0}:\mathbf{M_0}\,\mathbf{Q}_2+(\mathbf{Q_2}:\mathbf{M}_0+\mathbf{Q}_0:\mathbf{Q_2})\mathbf{M}_0\right)\\
\overline{\mathbf{r}}(\mathbf{Q}_0,\mathbf{Q}_1) &= \tilde{\mathbf{\Omega}}\cdot\mathbf{Q_1}-\mathbf{Q_1}\cdot\tilde{\mathbf{\Omega}}+a\,\left(\tilde{\mathbf{D}}\cdot\mathbf{Q_1}+\mathbf{Q_1}\cdot\tilde{\mathbf{D}}\right)\\
&\quad -2\,a\,\left(\tilde{\mathbf{D}}:\mathbf{M_0}\mathbf{Q}_1+\tilde{\mathbf{D}}:\mathbf{M_1}\mathbf{M}_0\right)+N\,\mathbf{Q}_1\cdot\mathbf{Q}_1\\
&\quad -N\,\left((\mathbf{Q}_1:\mathbf{M_0}+\mathbf{Q_0}:\mathbf{Q}_1)\mathbf{Q}_1+\mathbf{Q}_1:\mathbf{Q}_1\mathbf{M}_0\right)\,.
\end{aligned} \tag{50}$$

The solvability condition for $\mathbf{Q}_2$ therefore is

$$\mathbf{r}(\mathbf{Q}_0,\mathbf{Q}_1)\perp\mathcal{N}(\overline{\mathbf{A}}^T(\mathbf{Q}_0,\mathbf{Q}_1))\,. \tag{51}$$

B Analysis of the steady solvability conditions

We outline the analytical results summarized in the text.

B.1 The isotropic branch

For the isotropic branch, $\mathbf{Q}_0=\mathbf{0}$. from equations (19), (20), we get

$$\mathbf{A}(\mathbf{Q}_0)=(1-\frac{N}{3})\mathbf{I},\qquad \mathbf{r}(\mathbf{Q}_0)=\frac{2}{3}\,a\,\tilde{\mathbf{D}}\,. \tag{52}$$

Obviously, if $N\neq 3$, equation (18) always has a *unique solution* for $\mathbf{Q}_1$:

$$\mathbf{Q}_1=\frac{2\,a}{3-N}\,\tilde{\mathbf{D}}\,. \tag{53}$$

B.2 The stable nematic equilibrium branch

B.2.1 Persistence of logrolling states: $\theta = 0$

In this case, $\mathbf{Q}_0$ is diagonal:

$$\mathbf{Q}_0 = diag(-\frac{s}{3}, \quad -\frac{s}{3}, \quad \frac{2s}{3})\,. \tag{54}$$

The matrix A in (21) simplifies to:

$$\begin{pmatrix} \frac{s}{1-s} & 0 & 0 & -\frac{2s}{1+2s} & 0 \\ 0 & \frac{3s}{(1-s)(1+2s)} & 0 & 0 & 0 \\ 0 & 0 & 0 & 0 & 0 \\ -\frac{2s}{1+2s} & 0 & 0 & \frac{s}{1-s} & 0 \\ 0 & 0 & 0 & 0 & 0 \end{pmatrix}. \tag{55}$$

The transpose of r is

$$r^T = \Big(0, \quad \frac{1}{3}\,a\,(1-s), \quad 0, \quad 0, \quad 0\Big)\,. \tag{56}$$

The eigenvalues of A^T are explicit:

$$\frac{3s}{(1-s)(1+2s)}, \quad \frac{3s}{(1-s)(1+2s)}, \quad \frac{s(4s-1)}{(1-s)(1+2s)}, \quad 0, \quad 0\,, \tag{57}$$

with corresponding eigenvectors

$$(-1,0,0,1,0), \quad (0,1,0,0,0), \quad (1,0,0,1,0), \quad (0,0,0,0,1), \quad (0,0,1,0,0). \tag{58}$$

(The third eigenvalue can also be zero if $s = \frac{1}{4}$, i.e., $N = \frac{8}{3}$.) The solvability condition (22) is explicitly satisfied *unconditionally*, i.e., for all $N \geq \frac{8}{3}$ (i.e., $\frac{1}{4} \leq s < 1$) and for all aspect ratios with $a \in [-1, 1]$.

To prove the $O(Pe)$ correction to $\mathbf{Q}_0$ is logrolling, we find $Q_1(xx), Q_1(xy)$ and $Q_1(yy)$ explicitly from the solvability condition (22), and then go over to the solvability condition (51) for the second order solution $\mathbf{Q}_2$ to get $Q_1(xz) = Q_1(yz) = 0$. The expression of $\mathbf{Q}_1$ is shown in (27).

B.2.2 Persistence of in-plane flow-aligning states: $\theta = \frac{\pi}{2}$

The matrix A in (21) now is asymmetric depending on trigonometric functions of ϕ. Nonetheless, the eigenvectors of A^T are explicit:

$$\begin{aligned} v_1 &= (0, \quad 0, \quad -\sin\phi, \quad 0, \quad \cos\phi)\ , \\ v_2 &= (3-\cos 2\phi, \quad -2\sin 2\phi, \quad 0, \quad 3+\cos 2\phi, \quad 0)\ , \\ v_3 &= \left(\cos^2\phi, \quad \sin 2\phi, \quad 0, \quad \sin^2\phi, \quad 0\right)\ , \\ v_4 &= (\sin 2\phi, \quad -2\cos 2\phi, \quad 0, \quad -\sin 2\phi, \quad 0)\ , \\ v_5 &= (0, \quad 0, \quad -\cos\phi, \quad 0, \quad \sin\phi)\ , \end{aligned} \tag{59}$$

with corresponding eigenvalues

$$\frac{3s}{(1-s)(1+2s)}, \quad \frac{3s}{(1-s)(1+2s)}, \quad \frac{s(4s-1)}{(1-s)(1+2s)}, \quad 0, \quad 0, \tag{60}$$

respectively. The vector r in (21) becomes

$$r = \frac{1}{6}\begin{pmatrix} s\,\sin 2\phi\,(3 + a\,(1-s) - 3\,a\,s\,\cos 2\phi) \\ -3\,s\cos 2\phi + \frac{1}{2}\,a\ (4 + 2\,s - 3\,s^2 + 3\,s^2\,\cos 4\phi) \\ 0 \\ s\,\sin 2\phi\left(-3 + a - a\,s + 3\,a\,s\,\sin^2\phi\right) \\ 0 \end{pmatrix}. \tag{61}$$

Since the third eigenvalue above is also zero if $s = \frac{1}{4}$ ($N = \frac{8}{3}$), we have to distinguish $N = \frac{8}{3}$ from $N > \frac{8}{3}$.

If $N > \frac{8}{3}$, the eigenvectors v_4 and v_5 span the null space of A^T, so the solvability condition simplifies to $r^T v_4 = r^T v_5 = 0$. It is easy to see that $r^T v_5 = 0$ is unconditionally satisfied. After simplification, we get

$$r^T v_4 = s - \frac{1}{3}a\,(2+s)\,\cos 2\phi, \tag{62}$$

which produces the Leslie alignment angle (33) in weak shear for the Doi closure.

For infinite aspect ratios $|a| = 1$, the right hand side of (33) always has modulus less than 1. That is, we always can pick ϕ (there are two ϕ's of opposite sign) from (33) so that $r^T v_4 = 0$, and $\mathbf{Q}_1$ is solvable. For low aspect ratios, $0 < |a| < \frac{1}{3}$, the right hand side of (33) is always greater than modulus 1, and therefore *no solution exists* for $\mathbf{Q}_1$. For sufficiently large aspect ratios, $\frac{1}{3} < |a| < 1$, the right-hand-side of (33) will hit values ± 1 at a critical concentration N. The relationship between this critical concentration and the aspect ratio is discovered as $N_*(a)$ in (35). For $\frac{8}{3} < N \leq N_*(a)$, $\mathbf{Q}_1$ is solvable with exactly two Leslie angles of opposite sign. For $N > N_*(a)$, no solution exists for $\mathbf{Q}_1$.

For the special case $N = \frac{8}{3}$, the solvability conditions become

$$\begin{aligned} r^T v_3 &= \frac{3}{8} a \sin 2\phi = 0\,, & (63)\\ r^T v_4 &= \frac{1}{4}(1 - 3a \cos 2\phi) = 0\,, & (64) \end{aligned}$$

which can only be satisfied if $a = \frac{1}{3}$ and $\phi = 0$, or $a = -\frac{1}{3}$ and $\phi = \frac{\pi}{2}$.

To prove $Q_1(xz) = Q_1(yz) = 0$ (to show the perturbed solution is in-plane), we again go further to the solvability condition for $\mathbf{Q}_2$. With some manipulation of a combination of three linear and two quadratic equations, we are able to get the explicit expressions for $\mathbf{Q}_1$ for all $\frac{1}{3} \leq |a| \leq 1$, which is given in (35).

B.2.3 Out-of-plane flow-aligned states: $0 < \theta < \frac{\pi}{2}$

When $\theta \in (0, \frac{\pi}{2})$, the eigenvectors of A in the linear system (21) fall into two categories, first $\phi = \frac{\pi}{2}$ or $\frac{3\pi}{2}$, then all other ϕ are treated separately.

- **We begin with the case $\phi = \frac{\pi}{2}$ or $\phi = \frac{3\pi}{2}$.**

In this case, 0 is a double eigenvalue of A^T with corresponding eigenvectors

$$\begin{aligned} w_1 &= (\tan 2\theta, 0, 0, 2 \tan 2\theta, 2)\,, \\ w_2 &= (0, \tan\theta, 1, 0, 0)\,. \end{aligned} \qquad (65)$$

The right hand side of (20) is

$$r = \left(0, \frac{1}{6}(-2a(-1+s) + 3(1+a)s\sin^2 t), \frac{s}{4}(1+a)\sin 2t, 0, 0\right)\,. \qquad (66)$$

It is obvious that r is orthogonal to w_1. But the inner product of r and w_2 is

$$r^T w_2 = 3s + a(2+s)\,, \qquad (67)$$

which is never zero for s in $[\frac{1}{4}, 1)$ for $a > -\frac{1}{3}$. So, *no solution for* $\mathbf{Q}_1$ *exists.* For $-1 \leq a \leq -\frac{1}{3}$, let r be orthogonal to w_2, we get the boundary (35), the solid line in Figure 1, again.

- **Now we proceed to the case $\phi \neq \frac{\pi}{2}$ and $\phi \neq \frac{3\pi}{2}$.**

The five eigenvalues of $\mathbf{A}^T$ are explicitly given by:

$$0, \quad 0, \quad -2 + \frac{N}{4}(3 + \sqrt{1 - \frac{8}{3N}}), \quad \frac{N}{4}(1 + 3\sqrt{1 - \frac{8}{3N}}), \quad , \frac{N}{4}(1 + 3\sqrt{1 - \frac{8}{3N}}) \,. \tag{68}$$

The null space of A is 2-dimensional if $N > \frac{8}{3}$, spanned by

$$\begin{aligned} w_1 &= \begin{pmatrix} -3\sin 2\phi \sin 2\theta \\ (-1 + 3\cos 2\phi)\sin 2\theta \\ -4\sin\phi\,(2\cos^2\theta - \cos^2\phi\,\sin^2\theta) \\ 0 \\ 4\cos\phi\,(1 - \sin^2\theta\,\cos^2\phi) \end{pmatrix}, \\ w_2 &= \begin{pmatrix} \cos\phi\,(2\cos^2\theta - \sin^2\phi\,\sin^2\theta) \\ \sin\phi\,(1 - 2\sin^2\theta\,\sin^2\phi) \\ \csc^2\theta \sin\theta\,\cos\theta\,\cos 2\theta \\ \cos\phi\,(1 - \sin^2\theta\,\cos^2\phi) \\ 0 \end{pmatrix}. \end{aligned} \tag{69}$$

If $N = \frac{8}{3}$, the null space is 3-dimensional, spanned by w_1, w_2 above together with

$$w_3 = \begin{pmatrix} -(\cos 2\theta + \sin^2\phi\,\sin^2\theta) \\ \sin 2\phi\,\sin^2\theta \\ \cos\phi\,\sin 2\theta \\ -\cos^2\theta + \sin^2\theta\,\sin^2\phi \\ \sin\phi\,\sin 2\theta \end{pmatrix}. \tag{70}$$

We omit the long expression for r appearing in the equation (21), and record only the dot product of r with the null vectors w_1 and w_2:

$$\begin{aligned} r^T w_1 &= \tfrac{1}{6}\sin 2\theta\,[-9s - a(2+s) + 3(s + a(2+s))\cos 2\phi]\,, \\ r^T w_2 &= \tfrac{1}{6}\sin\phi\left[3\,s - 6\,s\,\sin^2\theta - a\,(2+s)(-1 + \sin^2\theta - \sin^2\theta\cos 2\phi)\right]. \end{aligned} \tag{71}$$

We distinguish the discussion between $|a|$=1 and $|a| < 1$.

$\star$ First consider the infinite aspect ratio case, $|a| = 1$.

If $\phi = 0$, then r is orthogonal to w_2, and from $r^T w_1 = 0$, we get $s = 1$ for $a = 1$, and $s = -\frac{1}{2}$ for $a = -1$, which are not in the allowable s-range $[\frac{1}{4}, 1)$. If $\phi \neq 0, \pi$, we set (71) to zero and solve for $\sin^2\theta$:

$$\sin^2\theta = \begin{cases} \frac{3\,(1+s)}{2(1+2\,s)}\,, & \text{for } a = 1 \\ \frac{3}{2(1-s)}\,, & \text{for } a = -1 \end{cases} \tag{72}$$

The modulus of the right hand of this expression is greater than 1 for s in the interval $[\frac{1}{4}, 1)$ Therefore, there is also no solution for θ for any finite N.

$\star$ Then consider finite aspect ratios, $|a| < 1$.

Suppose $\phi \neq 0, \pi$, and impose (71) must vanish. This yields:

$$\begin{aligned} \cos 2\phi &= \frac{9\,s + a\,(2+s)}{3(s + a\,(2+s))} && (73) \\ \sin^2\theta &= \frac{3\,(s + a\,(2+\ s))}{6\,s + 2\,a\,(2+s)}. && (74) \end{aligned}$$

From $0 < \sin^2\theta < 1$ $(\theta \neq 0, \frac{\pi}{2})$, one can deduce that the right hand side of the expression for $\cos 2\phi$ has modulus greater than 1. Therefore, there are no out-of-plane solutions for any $N \geq \frac{8}{3}$ when $\phi \neq 0, \pi$.

Now suppose $\phi = 0, \pi$. In this case, r is always orthogonal to w_2. The first equation in (71) simplifies to

$$r^T w_1 = -\frac{1}{3}((3-a)s - 2a)\sin 2\theta\,, \tag{75}$$

which never vanishes if $-1 \leq a < \frac{1}{3}$, so *no out-of-plane solution exists.* If $\frac{1}{3} < a < 1$, first impose that (71) vanishes, replace s by $s_+(N)$ from (14) and we arrive at an expression between N and the shape parameter a, which is identical to the boundary (35).

We complete the discussion by considering the case $N = \frac{8}{3}$, i.e., $s = \frac{1}{4}$ in the case $\phi = 0$ or π. Now, 0 is a triple eigenvalue, and the corresponding eigenvectors are w_1, w_2 and w_3 as shown earlier. It is trivial to check that the right hand side r is orthogonal to both w_2 and w_3. In order for r to orthogonal to w_1, the shape parameter a must equal to $\frac{1}{3}$.

B.3 Lower nematic solution branch

A similar analysis can be applied to the lower quiescent nematic branch, s_- in (14). Since these states are all unstable, we omit the mathematical details and only depict the results graphically in Figure 1(a), where the dotted, dashed curves mark the transition behavior.